Regulated expression and temporal induction of the tail-anchored sarcolemmal-membrane-associated protein is critical for myoblast fusion

Rosa M. GUZZO*, Jeffery WIGLE*, Maysoon SALIH*, Edwin D. MOORE† and Balwant S. TUANA*[1]

*Department of Cellular and Molecular Medicine, 451 Smyth Road, University of Ottawa, Ottawa, ON, Canada K1H 8M5, and †Department of Physiology, University of British Columbia, Vancouver, BC, Canada V6T 1Z3

Sarcolemmal-membrane-associated proteins (SLMAPs) define a new class of coiled-coil tail-anchored membrane proteins generated by alternative splicing mechanisms. An *in vivo* expression analysis indicated that SLMAPs are present in somites (11 days post-coitum) as well as in fusing myotubes and reside at the level of the sarcoplasmic reticulum and transverse tubules in adult skeletal muscles. Skeletal-muscle myoblasts were found to express a single 5.9 kb transcript, which encodes the full-length ~91 kDa SLMAP3 isoform. Myoblast differentiation was accompanied by the stable expression of the ~91 kDa SLMAP protein as well as the appearance of an ~80 kDa isoform. De-regulation of SLMAPs by ectopic expression in myoblasts resulted in a potent inhibition of fusion without affecting the expression of muscle-specific genes. Membrane targeting of the de-regulated SLMAPs was not critical for the inhibition of myotube development. Protein–protein interaction assays indicated that SLMAPs are capable of self-assembling, and the de-regulated expression of mutants that were not capable of forming SLMAP homodimers also inhibited myotube formation. These results imply that regulated levels and the temporal induction of SLMAP isoforms are important for normal muscle development.

Key words: myoblast fusion, sarcolemmal-membrane-associated protein, sarcoplasmic reticulum, skeletal differentiation, transverse tubule (T-tubule).

INTRODUCTION

Early in development, mesodermal cells are committed to a muscle cell fate in response to locally derived embryonic differentiation signals [1,2]. The withdrawal of determined myoblasts from the cell cycle is co-ordinated by the repression of growth-promoting genes coupled with the simultaneous induction of muscle-specific genes. Members of the family of basic helix–loop–helix myogenic regulatory factors, including MyoD, Myf5, myogenin and myogenic regulatory factor 4, predominantly control the specification and differentiation of skeletal muscles [3–5]. A hallmark feature of normal skeletal-muscle development is the fusion of mono-nucleated myoblasts to form fully differentiated, elongated multinucleated myotubes [6–8]. Morphologically, this process has been examined extensively in *Drosophila*, since myoblast fusion is complete in a matter of hours [9–13]. The process of myoblast fusion consists of various steps, including (i) cell–cell recognition of fusion-competent cells, (ii) cell–cell adhesion for close contact between fusion-competent cells, (iii) cell alignment and formation of prefusion complexes and (iv) the breakdown of membranes to remove excess membrane material [10,14]. Several protein classes play pivotal roles in this process, including cell-adhesion and cell-surface proteins (N-cadherins, M-cadherin, neural cell-adhesion molecule, integrins and disintegrins), cytoskeletal components and cytosolic signalling molecules [15–20]. Identification of the molecular components necessary for myoblast fusion would help us to understand better skeletal-muscle formation in developing and in regenerating adult skeletal muscles.

A key aspect of muscle differentiation is the formation of specialized membrane systems that play a central role in calcium regulation. These specialized membrane systems consist of sarcolemmal invaginations known as the T-tubules (transverse tubules) and the SR (sarcoplasmic reticulum), an extensive internal membrane compartment controlling the storage, release and uptake of intracellular calcium. Structural analyses have revealed that components of the SR and T-tubules are expressed early in development within muscle precursors at the prefusional stage [21–25]. Proper organization of these specialized membrane systems is essential for normal muscle development and function [26,27].

In an effort to identify the novel membrane components involved in EC (excitation–contraction) coupling, we previously cloned cDNAs encoding a family of α-helical coiled-coil proteins referred to as SLAPs (sarcolemmal-associated proteins) and were renamed as SLMAPs (sarcolemmal-membrane-associated proteins) [28,29]. The SLMAPs define a unique family of tail-anchored membrane proteins that exhibit developmental and tissue-specific expression [28,29]. Structural heterogeneity among SLMAP variants arises as a result of a combination of alternative splicing and alternative start-site usage of a single gene assigned to the human chromosome 3p14.3-21.2. Detailed sequence analyses revealed that SLMAPs share C-terminal sequences characterized by an extensive coiled-coil structure containing two LZ (leucine zipper) motifs believed to play a role in protein–protein interactions. Alternative splicing at the C-terminus generates SLMAP variants having unique TM domains (transmembrane domains), which target SLMAPs to cellular membranes [29]. In the present study, we have investigated the developmental expression of SLMAP in skeletal muscles and have used an *in vitro* model of skeletal-muscle differentiation to examine whether SLMAP plays a role in myogenesis. Our results

Abbreviations used: AD, activation domain; CAT, chloramphenicol acetyl-CoA transferase; d.p.c., days post-coitum; DHP, dihydroxypyridine; DNA-BD, DNA-binding domain; EC, excitation–contraction; GFP, green fluorescent protein; LZ, leucine zipper; MyHC, myosin heavy chain; PFA, paraformaldehyde; SLMAP, sarcolemmal-membrane-associated protein; SR, sarcoplasmic reticulum; TM domain, transmembrane domain; T-tubules, transverse tubules.

[1] To whom correspondence should be addressed (e-mail btuana@uottawa.ca).

suggest that SLMAP is expressed in early somites and may be important in myoblast fusion and in the membrane biology of EC coupling in developing muscles.

EXPERIMENTAL

Cell culture and transfection

Proliferating C2C12 myoblast cells were maintained at 37 °C in Dulbecco's modified Eagle's medium, supplemented with 10 % (v/v) heat-inactivated foetal bovine serum, 50 units/ml penicillin and 50 μg/ml streptomycin and gentamicin. Confluent C2C12 cultures were induced to differentiate by replacing the growth medium with Dulbecco's modified Eagle's medium containing 2 % (v/v) horse serum. For the stable expression of 6Myc–SLMAP fusion proteins, C2C12 cells were transfected with LIPOFECTAMINE Plus™ (Gibco BRL) or Fugene (Roche) transfection reagents according to the manufacturer's instructions. Myoblasts transfected with 6Myc-pcDNA3 served as controls. Individual G418-resistant clones were subsequently assayed for the expression of exogenous SLMAP protein by immunoblot analysis. The level of exogenous SLMAP protein was quantified relative to endogenous SLMAP by densitometry.

Immunohistochemistry

Timed pregnant mice were killed by lethal injection of sodium pentobarbital. Embryos [11–15 d.p.c. (days post-coitum)] were removed, rinsed in PBS and then fixed in 4 % (w/v) PFA (paraformaldehyde) in 0.1 M phosphate buffer (pH 7.4). Embryos were incubated overnight in a cryoprotectant [20 % (w/v) sucrose in PBS] at 4 °C. Fixed embryos were embedded in Tissue-Tek O.C.T. compound, frozen and stored at − 80 °C. Cryosections (6–10 μm) were collected on gelatin-coated microscope slides and stored at − 80 °C. Older embryos (18 d.p.c.) and adult tissues were isolated, rinsed in PBS, embedded in Tissue-Tek O.C.T. compound and then frozen. Cryosections were mounted on to slides and fixed overnight in 4 % PFA. PFA-fixed sections were washed with PBS, treated with 50 mM ammonium chloride in PBS for 5 min to reduce the non-specific staining of blood proteins. Sections were blocked in PBS containing 10 % (v/v) goat serum, 1 % Triton X-100 and 10 % (w/v) BSA for 20 min at room temperature (21 °C) before incubation with the primary antibodies (1 h, room temperature). After several washes with PBS, sections were incubated in PBS containing 5 % goat serum, 1 % Triton X-100 and the appropriate fluorochrome-linked secondary antibodies for 1 h at room temperature. After several washes with PBS, sections were mounted with anti-fading solution (Molecular Probes) and examined by either conventional microscopy or confocal microscopy.

In a series of experiments, coverslips were covered with 90 % (v/v) glycerol, 10 % (v/v) 10 × PBS (137 mM NaCl/8 mM NaH_2PO_4/2.7 mM KCl/1.5 mM KH_2PO_4, pH 7.4), 2.5 % (w/v) triethylenediamine and 0.02 % NaN_3, to which fluorescent microspheres (0.2 μm diameter; Molecular Probes) labelled with FITC and Texas Red had been added. The microspheres are fiduciary markers and permit accurate alignment of the three-dimensional datasets. A series of two-dimensional images were acquired through the cells at 0.25 μm spacing using a Nikon Diaphot 200 microscope and a Planapo 60/1.4 objective (pixel dimensions, 100 nm × 100 nm) [30]. The point spread function of the microscope was measured using fluospheres of the appropriate colour (0.1 μm diameter; Molecular Probes). Images were prepared, deconvolved and analysed as reported previously [31].

Antibodies

Anti-SLMAP(C) rabbit antibodies were raised against the C-terminal 370 amino acids of SLMAP, as described previously [28]. The antibodies used included anti-myogenin monoclonal antibody (Pharmingen, San Diego, CA, U.S.A.), anti-α-tubulin monoclonal antibody (clone DM 1A; Sigma–Aldrich), anti-myosin heavy-chain monoclonal antibody MF20 (Dr David Parry, University of Ottawa), anti-caveolin 3 monoclonal antibody (Transduction Laboratories, Lexington, KY, U.S.A.), anti-α-actinin 2 monoclonal antibody (Sigma–Aldrich), anti-α1 DHP (dihydroxypyridine) receptor monoclonal antibody (Chemicon, Temecula, CA, U.S.A.) and anti-Ca^{2+}-ATPase monoclonal antibody (Developmental Studies Hybridoma Bank, University of Iowa, Iowa, IA, U.S.A.). Rhodamine-RedX-conjugated mouse secondary antibody (Jackson ImmunoResearch Laboratories, Mississauga, ON, Canada), Alexa-Fluor 594-conjugated mouse secondary antibody (Molecular Probes) and Alexa-Fluor 488-conjugated rabbit secondary antibodies (Molecular Probes) were used in immunohistochemistry studies. Secondary antibodies used in immunoblotting experiments included anti-rabbit IgG–peroxidase-linked whole antibody (Amersham Biosciences) and peroxidase-conjugated AffiniPure goat anti-mouse IgG (Jackson ImmunoResearch Laboratories).

Immunofluorescence microscopy

Samples were visualized using an Axiophot (Carl Zeiss, Thornwood, NY, U.S.A.) microscope equipped with a 3CCD colour video camera. An Olympus IX70 laser-scanning inverted microscope with a × 63 oil immersion objective was used. Images were obtained using the Bio-Rad MRC 1024 confocal. The images were digitally processed using Northern Eclipse (version 5.0; Empix Imaging, Mississauga, ON, Canada) acquisition software as well as the Confocal Assistant 40 software. Images were processed further using Adobe Photoshop™ 5.0.

Northern-blot analysis

Total RNA was extracted from proliferating and differentiating C2C12 cells using TRIzol® reagent (Roche Molecular Biochemicals) according to the manufacturer's instructions. RNA was electrophoresed on 1 % agarose and 2.2 % (v/v) formaldehyde denaturing gel and transferred to a positively charged nylon membrane (Roche Molecular Biochemicals), which was probed with digoxigenin-labelled (Roche Molecular Biochemicals) cDNA probes for SLMAP, myogenin and glyceraldehyde-3-phosphate dehydrogenase and processed as described in [28,29].

Immunoblot analysis

Cultured cells were lysed in RIPA buffer (10 mM Tris/HCl, pH 7.4/1 mM EDTA/300 mM NaCl/1 % Nonidet P40/0.1 % SDS/1 % sodium deoxycholate), supplemented with a protease inhibitor cocktail (Sigma–Aldrich). Particulate material and unbroken cells were removed by centrifugation at 10 000 ***g*** for 10 min at 4 °C. The protein content of clarified lysates was determined using the BCA (bicinchoninic acid) protein assay kit (Pierce). Protein extracts were resolved by SDS/PAGE (10 % gel), electrotransferred on to PVDF membranes (Roche Molecular Biochemicals) and immunoblotted using the enhanced chemiluminescence detection system as described previously [28]. Densitometric analysis was performed using the Scion Image software (Scion Corp., Frederick, MD, U.S.A.) based on the NIH Image program.

SLMAP expression plasmids

SLMAP3M1 (nt 1–2337) was PCR-generated from the SLMAP rabbit cDNA clone (GenBank® accession no. U21157) using the forward primer SLMAPN-F (GGAATTCGATGCCGTCAGCCTTGGC) and the reverse primer SLMAPN-R (GATGCCAGCTTCTAGAGGGAGGACG). PCR products were inserted into the *Eco*RI and *Xba*I sites of the pcDNA3 mammalian expression plasmid (Invitrogen) in-frame with the 6Myc epitope tag. Sites of ligations were confirmed by DNA sequencing. The 6Myc-tagged ΔNSLMAP expression construct, encompassing the *Bgl*III–*Xba*I-digested SLMAP3 restriction fragment (lacking the first 315 amino acids of SLMAP3), was generated as described by Wigle et al. [28]. 6Myc-tagged SLMAP1 expression constructs encoding the TM2 domain or the construct lacking both the TM domains were generated by the method of Wielowieyski et al. [29]. The LZ mutant (SLMAPΔLZ) was generated by digesting 6Myc-SLMAP1-pcDNA3 with *Bam*HI. This digestion removed the segment of SLMAP that encoded the LZs (nucleotides 1790–2001). Nucleotides 2001–2314 of SLMAP3M1 (designated SLMAP3′) in pcDNA3 were retained for subsequent ligation. A PCR amplicon of 6Myc–SLMAP1 lacking the LZs was PCR-generated from the 6Myc-SLMAP1-pcDNA3 template using the 5′-primer (GAATTCAATGGATGAGCAAGACCT; 6Myc–SLP15′) and the 3′-primer (CGGATCCCTCTTTCTGCTGGTCCTCACACTGC; lacking the LZs). The PCR product (lacking the LZs) was restriction-digested (*Bam*HI) and then ligated into SLMAP3′. The GFP (green fluorescent protein)-tagged SLMAP (GFP–SLMAP) construct, which lacked the first 315 amino acids of SLMAP3, was generated using a *Bgl*III–*Xba*I-digested SLMAP3 restriction fragment inserted into GFP-pcDNA3.

Determination of the fusion indices

Fusion indices were determined for individual clones and control cells after 6 days in differentiation medium. Each G418-selected clone was initially seeded at 8.0×10^5 cells/60 mm plate and induced to differentiate when confluent. Cells were fixed in 4 % PFA and then stained with Harris haematoxylin/0.2 % acetic acid and counterstained in eosin solution. A minimum of 12 random fields was assayed for each clone. The total number of nuclei per field and the number of nuclei (three or more) per myotube were counted and fusion indices were calculated as (number of nuclei in myotubes/total number of nuclei in each field) × 100. The fusion index for each clone was taken as means ± S.D. for the mean fusion index and the significance of the results relative to control cells was determined by ANOVA.

Immunoprecipitations

C2C12 cells transiently transfected with GFP and 6Myc expression constructs were lysed 36 h post-transfection with RIPA buffer as described above. To eliminate non-specific interactions, clarified cell lysates were precleared with Protein A/G Plus–agarose-conjugated beads (Santa Cruz Biotechnology) for 15 min at 4 °C with constant rotation. Precleared lysates were retained and protein content was measured. For each immunoprecipitation condition, 350 μg of total protein was used and samples were diluted to 1:1 in PBS. Immunoprecipitations were performed by incubating the lysates with anti-myc 9E10 monoclonal antibodies (1:100) or purified rabbit IgGs or beads only overnight at 4 °C with constant rotation. Immunocomplexes were captured with the addition of equivalent amounts of prewashed Protein A/G Plus–agarose-conjugated beads to each sample for 4 h at 4 °C. Immunoprecipitated proteins bound to the Protein A/G–agarose beads were washed extensively and then resuspended in 2 × SDS/PAGE loading buffer. Immunocomplexes were eluted from the Protein A/G–agarose beads by boiling, resolved by SDS/PAGE and subjected to immunoblot analysis.

In vivo interaction assay

Sequences encoding the first 454 amino acids of SLMAP (SLMAPN) were generated by PCR amplification of full-length SLMAP rabbit clone (GenBank® accession no. U21157) using the primers 5′-GGAATTCATGCCGTCAGCCTTGGCCATC and 3′-CGAATTCACAGAAGGGACAAGCTGAG. Primers 5′-GGAATTCGATGCCGTCAGCCTTGGC and 3′-GATGCCAGCTTCTAGAGGGAGGACG were used to PCR-amplify the SLMAP sequence encoding amino acids 454–775 (SLMAPC). SLMAPC cDNA with LZ deletions (amino acids 597–667; SLMAPCΔLZ) was amplified from template SLMAP3M1ΔLZ using the primers 5′-GGGAATTCATGGATGAGCAAGACCTG and 3′-CCGTCTAGATCATTGGAGCAGCTTCAGGTTGTC. The SLMAPN PCR product was *Eco*RI–*Bam*HI-digested and the SLMAP-C and SLMAP-CΔLZ PCR products were *Eco*RI–*Xba*I-digested. Digested SLMAP products were used for insertion into the same sites of (i) pM in-frame with the GAL4 DNA-binding domain (DNA-BD) or (ii) pVP16 activation domain (AD) vector (Mammalian Matchmaker Two Hybrid Assay kit; Clontech, BD Biosciences Canada, Mississauga, ON, Canada).

Subconfluent C2C12 myoblasts grown on 60 mm plates were co-transfected with 1 μg of mammalian CAT (chloramphenicol acetyl-CoA transferase) reporter vector (pG5CAT) containing five consensus GAL4-binding sites, 1 μg of the β-galactosidase expression plasmid (pCMV-LacZ) and 2 μg of recombinant plasmids derived from pM and pVP16 (Clontech) using the LIPOFECTAMINE Plus™ transfection reagent (Gibco BRL). For a positive control (sample 14), cells were co-transfected with 1 μg of pG5CAT, 1 μg of pCMV-LacZ, 1 μg of pVP16-T (VP16 AD to SV40 target antigen known to interact with p53) and 1 μg of pM53 (fusion of GAL4 DNA-BD to mouse p53 protein). Cells were lysed, 48 h after transfection, in 0.25 M Tris/HCl (pH 7.8) and centrifuged at 10 000 ***g*** for 10 min. Samples were heated to 65 °C for 10 min, cooled on ice and then combined with CAT assay buffer (135 mM Tris, pH 7.8/1.6 mM chloramphenicol/0.74 μCi of ^{3}H-acetyl CoA). Mixtures were heated to 37 °C for 1 h and extracted with ice-cold ethyl acetate. Extracts were centrifuged at 10 000 ***g*** for 10 min and the aqueous phase was retained for quantifying the radioactivity (^{3}H) using a liquid-scintillation counter. The levels of CAT activity were normalized to the β-galactosidase activity in the respective cell extracts. Basal CAT activity (sample 1 control) was set as 1 and the fold induction of CAT activity was calculated as c.p.m. (samples 2–14)/basal CAT activity.

RESULTS

SLMAP expression in developing skeletal muscles

As a first step towards understanding the function of SLMAPs in skeletal muscles, we examined the *in vivo* distribution of SLMAP in developing and mature skeletal muscles. SLMAP antibodies [28] were used to detect SLMAP localization in cryosections of tissue from developing mice (11–18 d.p.c.) as well as in adult skeletal muscles (Figure 1). As illustrated in Figure 1(A), SLMAP expression was detected in developing somites at 11 d.p.c. Early in development (11–13 d.p.c.), SLMAP labelling was primarily observed at punctate clusters along the

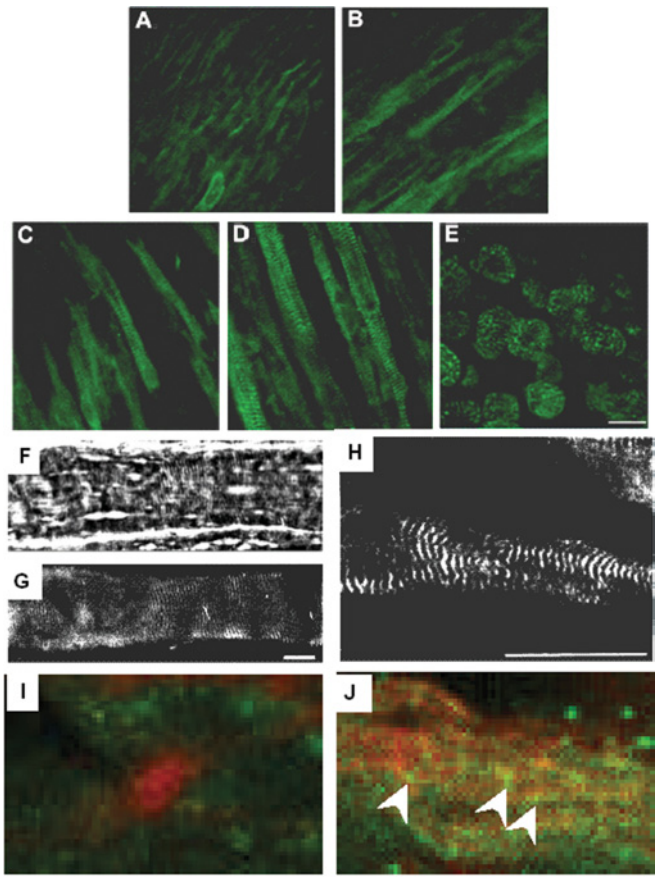

Figure 1 SLMAP expression in developing and adult skeletal muscles

Formalin-fixed frozen sections (6–10 μm) of mouse embryos at stages 11 d.p.c. (**A**), 13 d.p.c. (**B**), 15 d.p.c. (**C**) and 18 d.p.c. (**D**, **E**) were labelled with anti-SLMAP rabbit polyclonal antibodies [28]. SLMAP antibodies labelled the somites (**A**) as well as punctate structures in longitudinal sections of skeletal muscles at 13 d.p.c. (**B**). At 18 d.p.c., SLMAP staining was detected within reticular formations in longitudinal (**D**) and transverse (**E**) sections. Absorbance of sections, 0.5 μm. Confocal images show SLMAP distribution along transverse bands in longitudinal cryosections of adult rat tibialis anterior muscles (**G**, **H**). Confocal images of SLMAP (green) and golgin 58 (red, **I**) and endoplasmic reticulum/SR calcium-ATPase (red, **J**) at 15 d.p.c. Scale bar, 25 μm.

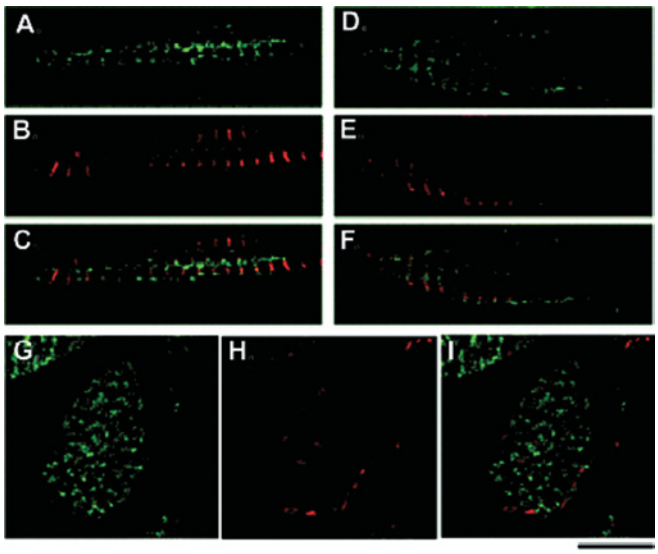

Figure 2 Distribution of SLMAP relative to myofibril arrangement in developing and adult skeletal muscles

At 18 d.p.c. (**A**–**E**), SLMAP antibodies (**A**, **D**) stained the structures flanking the α-actinin-stained Z-line (**B**, **E**). When confocal images were overlaid (**C**, **F**), SLMAPs were observed within structures surrounding the myofibrils. In transverse cryosections of adult soleus muscles, SLMAP antibodies (**G**) labelled the structures flanking the Z-line stained with α-actinin (**H**). Merging of SLMAP and α-actinin signals is shown in (**I**). Scale bar, 10 μm. Absorbance of sections, 0.5 μm.

length of the myotube (Figures 1A and 1B). Before the myotube-to-myofibre transition (15 d.p.c.), SLMAP distribution became increasingly well organized and was abundant at reticular formations and fine longitudinal structures (Figure 1C). This SLMAP-specific staining pattern was evident in skeletal muscles examined at later stages in development (18 d.p.c.; Figures 1D and 1E) and was also observed in adult tibialis anterior muscles (Figures 1F–1H).

To examine more closely the subcellular localization of SLMAPs in developing and skeletal muscles, double-immunofluorescent labelling was performed using various muscle-specific antibodies. To define better the punctuate staining pattern of SLMAP seen in early muscle development (Figure 1), we found that anti-SLMAP did not co-localize with the Golgi marker golgin 58 (Figure 1I), but did co-localize, in part, with endoplasmic reticulum/SR marker early development (Figure 1J). We then examined the arrangement of SLMAPs relative to myofibril components by co-staining with α-actinin 2, an actin filament-cross-linking molecule present at the Z-line of myofibrils. Staining with the Z-line marker revealed a clear striated pattern that was distinct from SLMAP at 18 d.p.c. (Figures 2A and 2D), which was clearly associated with distinct structures flanking the myofibril Z-line (Figures 2B and 2E). At 18 d.p.c. as well as in mature adult skeletal muscles (Figures 2G–2I), the majority of SLMAP labelling was distinct from that of α-actinin and was primarily detected as a continuous network around and between the myofibrils and also as fine longitudinal structures orientated perpendicular to the Z-line.

In longitudinal and transverse cryosections of developing skeletal muscles (18 d.p.c.) and adult skeletal muscles, SLMAP co-localized with the Ca^{2+}-ATPase, a marker of the longitudinal SR membrane system (Figures 3A–3F). SLMAP co-distribution with the SR marker was observed within clusters in transverse cryosections of developing skeletal muscles (18 d.p.c.; Figures 3A–3C) and adult soleus muscles (Figures 3D–3F). In longitudinal cryosections (18 d.p.c.), SLMAP and the Ca^{2+}-ATPase were co-localized at cross-striations along the length of the myofibres (Figures 3A–3C). To determine the localization of SLMAP relative to the T-tubules, dual immunostaining was performed using antibodies against the α-1 subunit of the DHP receptor (Figures 3G–3I). Consistent with the mature organization of T-tubules, the membrane labelled with αs-1 DHP receptor antibody clusters in transverse cryosections of adult muscles (Figures 3G–3I). Some co-localization of the DHP receptor was evident with SLMAP as yellow staining (Figures 3I). A combination of deconvolution and three-dimensional image analyses of muscle sections labelled with SLMAP antibodies and the DHP receptor (Figure 3J) and the surface membrane marker anti-caveolin-3 [52] (Figure 3K) demonstrated that SLMAP localized to discrete regions in the cellular interior and at the cell's periphery. By deconvolution microscopy, there is some co-localization of SLMAP with caveolin-3 (Figure 3K) and also with the DHP receptor (Figure 3J) as indicated by the white voxels. Taken together, the above results indicate that SLMAP is a component of both the surface membrane and the SR.

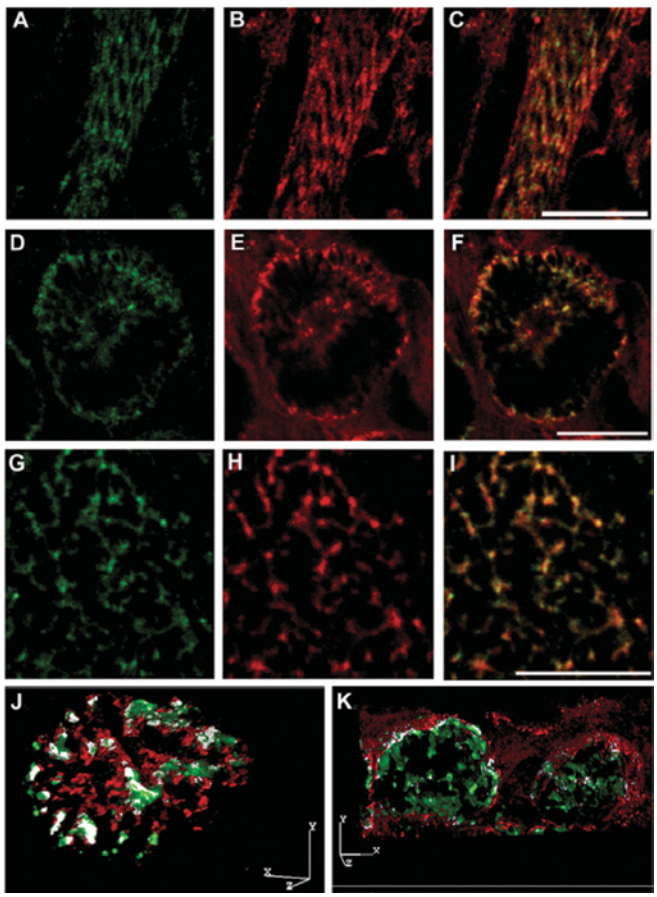

Figure 3 SLMAP localization relative to membrane structures

Co-localization of SLMAP (**A**, **D**) with the SR Ca^{2+}-ATPase (**B**, **E**) was observed in skeletal muscles at 18 d.p.c. (**A**–**C**) and adult soleus muscles (**D**–**F**). Merging of SLMAP and Ca^{2+}-ATPase is shown in (**C**, **F**). The α1-subunit of the DHP receptor antibody (**H**, **K**) identified T-tubules in adult soleus muscles. Regions of DHP receptor co-localization with SLMAP (**G**, **J**) are shown in yellow (**I**). Scale bar, 10 μm. Skeletal muscles (18 d.p.c.) co-stained with SLMAP (green) and DHP receptor (red) are shown in (**J**). Skeletal muscles (18 d.p.c.) co-stained with SLMAP (green) and caveolin-3 (red) are shown in (**K**). Confocal images shown in (**J**, **K**) are three-dimensional reconstructions of a depth of 7.75 μm. Co-localized voxels are shown in white. Scale bar, 5 μm in each dimension.

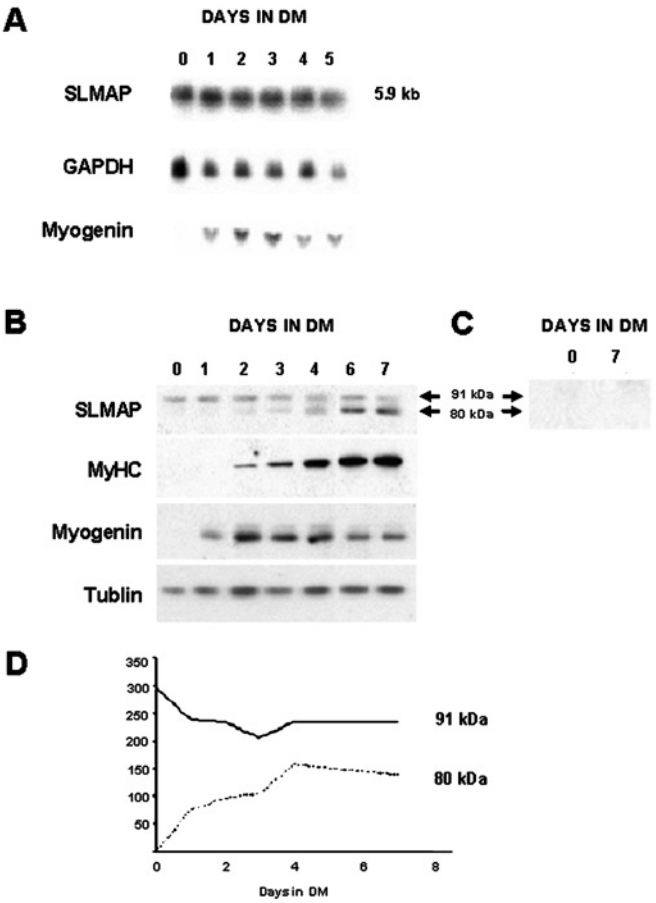

Figure 4 SLMAP transcript and protein expressions during myogenic differentiation

(**A**) SLMAP mRNA expression in C2C12 myoblasts (lane 0) and differentiated C2C12 myotubes on various days (lanes 1–5) after mitogen depletion. The 5.9 kb SLMAP transcript is expressed in undifferentiated (lane 0) and differentiating C2C12 cells (lanes 1–5). Myogenin mRNA expression is initiated early in the differentiation programme (lanes 1–5). The glyceraldehyde-3-phosphate dehydrogenase (GAPDH) transcript is shown as a loading control. (**B**) Immunoblot analysis demonstrated that undifferentiated C2C12 cells express a 91 kDa SLMAP isoform (lane 0). An 80 kDa SLMAP isoform is induced after C2C12 differentiation (lanes 1–7). Skeletal-muscle-specific markers, myogenin and MyHC, are shown. α-Tubulin staining was used as a loading control. (**C**) Immunoabsorption of the SLMAP antibodies with bacterially expressed SLMAP proteins demonstrated antibody specificity for the 91 kDa SLMAP protein (lane 0) as well as the differentiation-induced 80 kDa SLMAP protein (lane 7). (**D**) Densitometric analysis of SLMAP expression levels during differentiation. Western blots represented in (**B**) were analysed using the Scion software. Densitometry values (in arbitrary units) were normalized with the α-tubulin levels measured for each time point. The results are representative of 2–3 independent experiments.

Induction of an ~ 80 kDa SLMAP isoform during muscle differentiation

In view of the observation that SLMAP is expressed early in developing skeletal muscles, we assessed whether the SLMAP transcript and protein levels are regulated during skeletal-muscle differentiation. The C2C12 myoblast cell line derived from mouse femoral muscle satellite cells is a well-established *ex vivo* model of skeletal-muscle differentiation [32,33]. In mitogen-rich media, C2C12 cells proliferate as myoblasts and can be induced to differentiate by withdrawal of serum from the culture medium. After mitogen depletion, myoblasts undergo biochemical and morphological differentiation as confirmed by the induction of muscle-specific gene expression and myoblast fusion to produce elongated multinucleated myotubes.

By immunoblot analysis, undifferentiated C2C12 myoblasts exclusively expressed a 91 kDa SLMAP protein (Figure 4B, lane 0). The previously characterized anti-SLMAP rabbit antibodies used were specific for the detection of SLMAP proteins by immunoblot analysis, since no signal was observed after immunoabsorption of SLMAP antibodies with bacterially synthesized SLMAP proteins (Figure 4C, lane 0). We investigated whether SLMAP transcript (Figure 4A) and protein levels (Figure 4B) are altered during the time course of myogenic differentiation. By Northern-blot analysis, the biochemical differentiation of C2C12 cells was monitored based on the induction of myogenin mRNA expression, since this bHLH transcription factor myogenin is expressed early in the skeletal-muscle differentiation programme and is critical for myoblast fusion [34–37]. Induction of myogenin mRNA expression was detected as early as 24 h after the removal of mitogens and its expression level increased as the differentiation programme progressed (Figure 4A). Morphological differentiation was verified on the basis of myotube formation, which occurred approx. 2 days after mitogen depletion. A 5.9 kb SLMAP transcript was expressed in

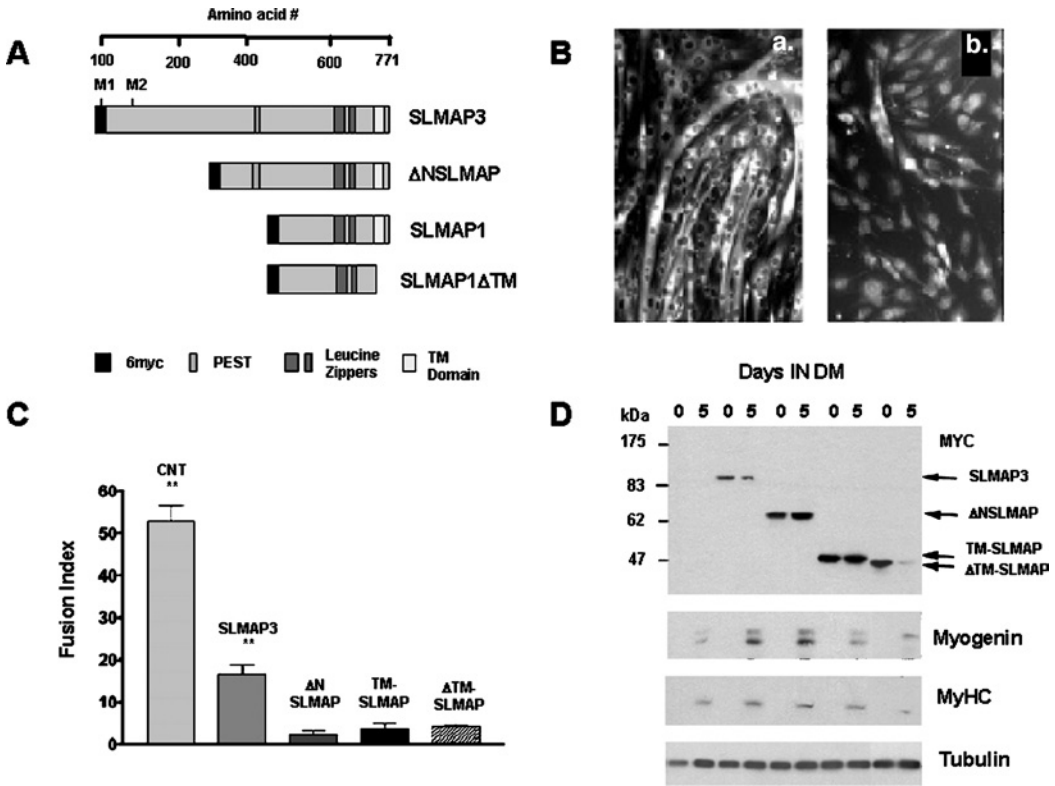

Figure 5 SLMAP overexpression affects the morphological differentiation of C2C12 myoblasts, but does not affect biochemical differentiation

(**A**) Schematic representation of the 6Myc-tagged SLMAP expression constructs used for stable transfections in C2C12 myoblasts. M1 and M2 refer to the two divergent initiating methionine residues identified in SLMAP3 [28]. (**B**) Haematoxylin–eosin-stained C2C12 clones at day 6 of differentiation after transfection with pcDNA (a) or SLMAP (b). (**C**) Reduced myotube formation was observed in C2C12 myoblasts stably transfected with 6Myc–SLMAP variants. Fusion indices were calculated from 3–4 individual clones for each construct after 6 days under differentiation-promoting conditions. Error bars represent S.D. for each transfectant. (**D**) Stable clones expressing 6Myc–SLMAP variants were monitored for the expression of differentiation markers on days 0 and 5 after mitogen removal. Expressions of 6Myc–SLMAP3 (102 kDa), 6Myc–ΔNSLMAP (72 kDa), 6Myc–TM-SLMAP (47 kDa) or 6Myc–ΔTM-SLMAP1 (42 kDa) were assayed using anti-myc monoclonal antibodies. Anti-myogenin monoclonal antibodies and anti-MyHC (MF20) monoclonal antibodies were used as markers of skeletal differentiation. Anti-α-tubulin antibodies were used as a control for equal loading.

undifferentiated C2C12 myoblasts and corresponds to the transcript encoding SLMAP3 (Figure 4A). No discernible change in the level of SLMAP transcript expression was detected during the course of differentiation, nor were other SLMAP transcripts expressed as the differentiation progressed.

SLMAP protein levels were next examined to determine whether SLMAP undergoes post-transcriptional regulation during differentiation. Whereas MyoD was expressed in differentiating myoblasts as well as in undifferentiated cells committed to the myogenic lineage (results not shown), myogenin protein expression was observed only after the induction of myotube formation (Figure 4B). The ubiquitous 91 kDa SLMAP isoform was expressed in both proliferating myoblasts and differentiated myotubes. Interestingly, SLMAP antibodies also recognized a differentiation-induced ~80 kDa protein (Figure 4B, lanes 1–7). Immunoabsorption of SLMAP antibodies with SLMAP fusion proteins further established the antibody specificity for the ~80 kDa SLMAP variant (Figure 4C, lane 7). Densitometric analysis confirmed that the expression level of the ~80 kDa SLMAP protein increased as differentiation progressed, whereas expression of the 91 kDa protein remained relatively constant (Figure 4D). To address the question of a specific link between the induction of the ~80 kDa SLMAP protein and cell-cycle withdrawal, SLMAP protein expression was examined in non-myogenic cell lines. Withdrawal from the cell cycle was induced in HeLa and NIH 3T3 fibroblast cells by culturing these cells under serum starvation conditions. The ~80 kDa SLMAP protein was not detected by immunoblot analysis of the protein extracts from serum-starved cells (results not shown).

Forced expression of SLMAP in myoblasts affects morphological differentiation

To assess whether the temporal induction of the SLMAP isoform was critical for myotube formation, we ectopically expressed SLMAP in C2C12 myoblasts and examined their ability to undergo biochemical and morphological differentiation. C2C12 myoblasts overexpressing SLMAP3 (6Myc–SLMAP3; Figure 5A) cultured for 6 days under differentiation-promoting conditions showed a significant reduction in the number of myotubes relative to the control transfectants (Figures 5B and 5C). Additional 6Myc–SLMAP variants were generated (Figure 5A), consisting of a variant lacking amino acids 1–315 of SLMAP3 (6Myc–ΔNSLMAP), SLMAP1 expressing the constitutively active TM domain (6Myc–SLMAP1-TM) as well as a TM domain mutant (6Myc–SLMAP1ΔTM). Consistent with the overexpression of the full-length molecule in myoblasts, forced expression of the membrane-associated SLMAP variants (6Myc–ΔNSLMAP, 6Myc–SLMAP1-TM) and the TM domain mutant (6Myc–SLMAP1ΔTM) elicited a significantly reduced (>90% inhibition) capacity for myotube formation (Figure 5C). The level of ectopically expressed SLMAP protein was quantified for each

individual clone and its level relative to endogenous SLMAP varied from 0.5- to 1.5-fold for the full-length SLMAP and from 1- to over 5-fold for the shorter deletion mutants. Irrespective of the level of SLMAP expression, each transfectant gave the same degree of inhibition of myoblast fusion. It should be noted that the control for these experiments represented myoblasts transfected with the 6Myc-pcDNA3 vector, and Myc-epitope-tagged proteins have also been used by other authors to study myoblast fusion and differentiation [30].

To determine whether the effect on fusion observed with SLMAP overexpression was attributed to defective biochemical differentiation, the expression of skeletal-muscle-specific proteins was monitored by immunoblot analysis. Expression of the early differentiation marker myogenin and muscle-specific MyHC (myosin heavy chain) was induced in each of the SLMAP-overexpressing clones (Figure 5D). The relative level of expression of these polypeptides in fusion-defective myoblasts with respect to the mock-transfected clones after day 5 of differentiation was 1.28 for MyHc and 0.99 for myogenin as quantified by densitometry. These results are representative of 2–3 individual clones that were isolated and assayed for each of the SLMAP-expressing constructs. Thus the fusion defects observed were not a consequence of the inhibition of biochemical differentiation; rather, these findings suggest that the regulated levels of SLMAPs are critical for the proper fusion of membranes.

SLMAP homodimerization is mediated by the leucine-rich coiled coils

Coiled-coil motifs are known to mediate protein oligomerizations and constitute a primary structural feature of the SLMAP polypeptides [28,29]. To assess the potential for SLMAP homodimerization, we performed co-immunoprecipitation experiments using C2C12 cells transfected with GFP- and 6Myc-epitope-tagged SLMAP polypeptides (Figure 6A). C2C12 cells were co-transfected with constructs encoding 6Myc–SLMAP3 (102 kDa) and the GFP–SLMAP variant (72 kDa; Figure 6B) or were co-transfected with constructs encoding the 6Myc–SLMAP1 variant (49 kDa) and the GFP–SLMAP variant (72 kDa; Figure 6C). Immunoblot analysis with monoclonal anti-myc antibodies confirmed the presence of the 102 kDa 6Myc–SLMAP3 protein (Figure 6B, right panel) as well as the 49 kDa 6Myc–SLMAP1 (Figure 6C, right panel) in lysates (lane L) of transfected cells. SLMAP antibodies recognized the 6Myc-tagged SLMAP proteins and the GFP–SLMAP variant (Figures 6B and 6C; left panel, lane L). Immunoblot analysis demonstrated that each of the 6Myc–SLMAP variants were specifically immunoprecipitated by anti-myc monoclonal antibodies (Figures 6B and 6C; right panel, lane M). Association of the 6Myc–SLMAP3 protein with the GFP–SLMAP protein was confirmed by immunoblot analysis using SLMAP antibodies (Figure 6B; left panel, lane M). The C-terminal sequences present in SLMAP are responsible for this interaction since 6Myc–SLMAP1 specifically precipitated the GFP–SLMAP protein (Figure 6C, left panel, lane M).

Previous sequence analyses of the C-terminal sequences conserved in each of the SLMAP isoforms have identified leucine-rich coiled-coil motifs [28]. Since this specialized form of coiled-coil structure is known to serve as an oligomerization motif, which can modulate protein activity in various proteins [38–41], we reasoned that the leucine-rich coiled-coil present in SLMAPs mediate SLMAP–SLMAP interactions. An *in vivo* interaction assay was therefore used to address this issue, whereby myoblasts were co-transfected with the CAT reporter construct and SLMAP variants encompassing N-terminal [SLMAP(N)] or C-terminal sequences [SLMAP(C)] fused to either the VP16 AD or the GAL4 DNA-BD (Figure 7A). Basal levels of reporter CAT activity were determined in lysates from control transfectants (Figure 7B, lanes 1–4). The level of CAT induction was similar to basal levels in cells co-transfected with either of the following: SLMAP(C) and SLMAP(N) constructs (Figure 7B, lane 6) fused to either AD or DNA-BD; SLMAP(N) and SLMAP(N) fused to either AD or DND-BD (Figure 7B, lane 5). A significant induction of CAT activity above basal levels (104-fold) was measured in lysates of cells co-transfected with the SLMAP(C)-AD and SLMAP(C)-DNA-BD constructs, confirming that the SLMAP C-terminus contains sequence information essential for SLMAP homodimerization (Figure 7B, lane 8). The leucine-rich coiled-coil mutant (SLMAPCΔLZ) failed to activate the expression of the CAT reporter gene above basal levels (Figure 7B, lanes 9–11). The leucine-rich coiled-coil motifs of an unrelated protein, ninein (GenBank® accession no. NM_008697), were fused to the GAL4 DNA-BD and co-transfected with C-terminal SLMAP sequences fused to the VP16 AD (Figure 7B, lane 12). These conditions did not result in the activation of CAT reporter expression and suggest that the leucine-rich coiled coil in SLMAP specifically mediates SLMAP–SLMAP associations.

Next, we assessed whether the fusion-defective phenotype observed in cells overexpressing SLMAP was attributed to inappropriate SLMAP homodimer formation. To address this issue, myoblasts were stably transfected with an SLMAP mutant lacking the leucine-rich coiled coil and were induced to differentiate as described in the Experimental section. Fusion indices were calculated for the mutant and control cells after 6 days in differentiation media. In the absence of SLMAP–SLMAP interactions, a fusion-defective phenotype was also observed in these (Figure 7C), thus indicating that de-regulation of SLMAP oligomerization is not responsible for the defective myotube formation.

DISCUSSION

Results of the present study indicate that SLMAP is expressed in a developmentally regulated manner and may play a role in myoblast fusion and membrane function during myogenesis. These studies reveal that SLMAP expression is initiated early during *in vivo* skeletal myogenesis and SLMAP proteins become distributed within specialized membrane systems involved in calcium signalling as development progressed. SLMAP expression was detected within somites at 11 d.p.c. when myogenic cells elongate and immature myofibrils appear [42]. SLMAP expression levels increased as the fusion process was initiated in the developing embryo (13 d.p.c.) [42], thus suggesting that regulated SLMAP levels may be required for this crucial morphological process in skeletal-muscle development. There appeared to be a direct link between the onset of myotube formation and the induction of the ~80 kDa SLMAP isoform. Appearance of the ~80 kDa SLMAP variant was observed only after the initiation of myotube formation and its expression is not a consequence of cell-cycle withdrawal since it was not expressed in non-myogenic cell lines forced to exit the cell cycle. These results indicate that the temporal appearance of SLMAP isoforms during skeletal myogenesis appears to be specific for the differentiation process. SLMAP mRNA expression levels remained unchanged during the course of differentiation and both myoblasts and myotubes were found to express a single 5.9 kb mRNA transcript. Post-transcriptional regulation of SLMAP may provide the specificity of expression required during differentiation. In this regard, two initiating methionine residues have been identified previously within SLMAP mRNA, which may account for the expression of the two different SLMAP isoforms observed during myotube formation [28].

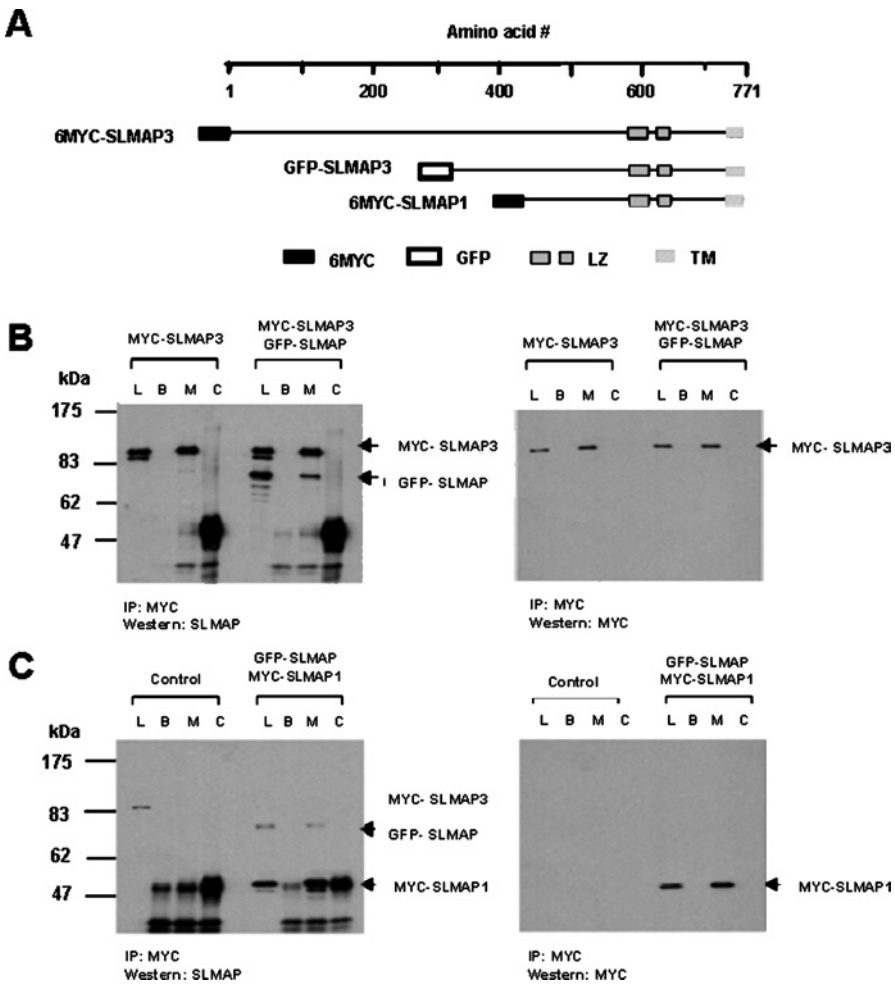

Figure 6 C-terminal SLMAP sequences direct SLMAP–SLMAP interactions

(**A**) Schematic representation of the 6Myc and GFP-tagged expression constructs used for transient transfections and immunoprecipitation studies. (**B**) C2C12 cells were transfected with 6Myc–SLMAP3 (MYC-SLMAP3) or co-transfected with 6Myc–SLMAP3 and GFP–SLMAP. The membrane blot shown in the left panel was immunoblotted with anti-SLMAP rabbit antibodies. In lysates (lane L), SLMAP antibodies detected the 91 kDa endogenous SLMAP as well as the ectopically expressed 6Myc–SLMAP3 (103 kDa) and the GFP–SLMAP (72 kDa) variant. In the right panel, myc antibodies detected only the 6Myc–SLMAP3 variant in lysates of transfected cells. Immunoprecipitations using myc antibodies specifically purified the 6Myc–SLMAP3 variant (right panel, lane M). Western-blot analysis using SLMAP antibodies further showed that the immunoprecipitated 6Myc–SLMAP3 protein complexed with the GFP–SLMAP protein (left panel, lane M). (**C**) C2C12 cells were co-transfected with 6Myc-pcDNA3 and GFP-pcDNA3 (controls) or co-transfected with 6Myc–SLMAP1 (MYC-SLMAP1) and GFP–SLMAP (GFP–SLMAP). The membrane shown in the left panel was immunoblotted with anti-SLMAP antibodies. In lysates of control cells, SLMAP antibodies detected only the 91 kDa endogenous SLMAP. SLMAP antibodies detected both the 6Myc–SLMAP1 (47 kDa) and the GFP–SLMAP (72 kDa) variant in lysates of transfected cells. In the right panel, myc antibodies detected only the 6Myc–SLMAP1 variant in lysates of transfected cells. Immunoprecipitation using myc antibodies specifically purified the 6Myc–SLMAP1 variant (right panel, lane M). Western-blot analysis using SLMAP antibodies also showed that the immunoprecipitated 6Myc–SLMAP1 complexed with GFP–SLMAP (left panel, lane M). Lane L, lysate; lane B, mock immunoprecipitation with Protein A/G–agarose beads; lane M, immunoprecipitation with anti-myc monoclonal antibody; lane C, control immunoprecipitation with rabbit IgGs. The results are representative of two independent experiments.

The de-regulation of SLMAP by ectopic expression in myoblasts seriously compromised the ability of these cells to fuse to myotubes under differentiation-promoting conditions. In spite of the impaired ability of SLMAP-overexpressing myoblasts to form multinucleated myotubes, these cells remained permissive for biochemical differentiation. The fusion defect appeared to be independent of SLMAP association with membranes since the expression of mutants lacking the C-terminal TM domain also impaired the ability of myoblasts to fuse. The primary structure of SLMAP revealed that it has extended coiled-coil regions that may be ideal for protein–protein interactions. Protein–protein interaction assays demonstrated that SLMAP proteins can self-assemble and these interactions are mediated by the leucine-rich coiled-coil motifs. Overexpression of SLMAP deletion mutants defective in the homodimerization domain also compromised the fusion of myoblasts. Thus the fusion-defective phenotype caused by the de-regulated expression of SLMAP in myoblasts strongly suggests that normal levels of the polypeptide and the temporal induction of SLMAP isoforms may play critical roles in the fusion of myoblasts.

The organized assembly of specialized membrane components (SR, T-tubules) relative to components of the contractile apparatus is a hallmark feature of the differentiated muscle structure and muscle function [27,43]. The distribution of SLMAP in developing and adult skeletal muscles indicated that it is a major component of the continuous membrane network around and between the myofibrils, consistent with the distribution of the SR and T-tubules. The observation that SLMAPs are distributed to SR and T-tubules suggests that SLMAPs may function as junctional membrane components that provide structural integrity, as has been described recently for junctophilin, another C-terminal anchored protein of the SR membrane, which binds the lipid

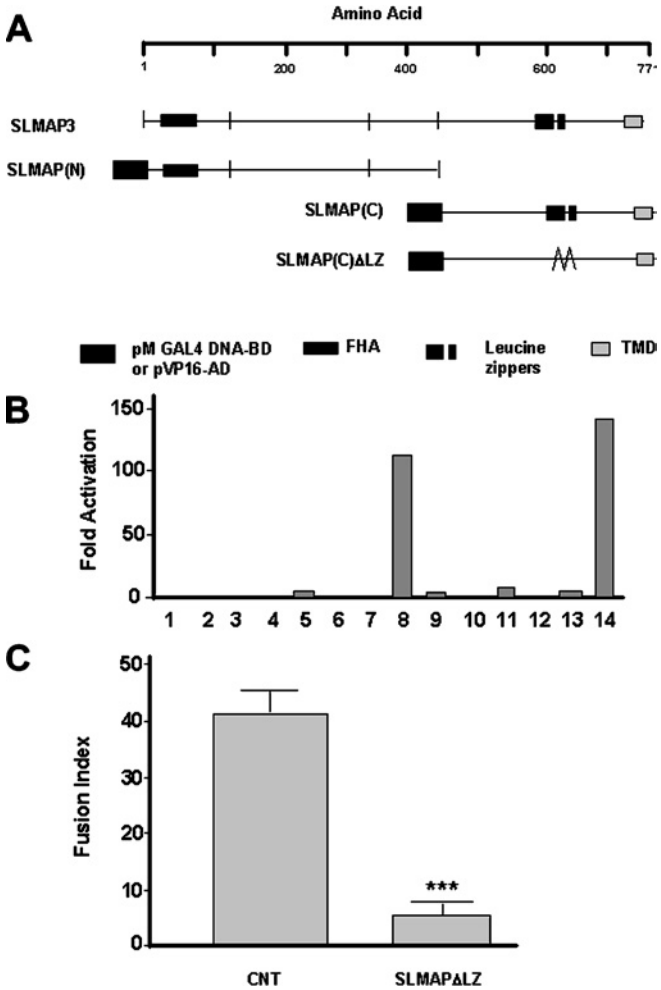

Figure 7 LZ motifs mediate SLMAP homodimer formation

(**A**) SLMAP3 sequences encoding amino acids 1–450 (SLMAPN) or 450–771 (SLMAPC) were fused in-frame with either the GAL4 DNA-BD or the VP16 AD. (**B**) C2C12 myoblasts were co-transfected with the CAT reporter plasmid pCMV-LacZ, the DNA-BD recombinant plasmid or the AD recombinant plasmid. Lane 1, DNA-BD + AD; lane 2, SLMAPN-(DNA-BD) + AD; lane 3, DNA-BD + SLMAPC-(AD); lane 4, SLMAPC-(DNA-BD) + AD; lane 5, SLMAPN-(DNA-BD) + SLMAPN-(AD); lane 6, SLMAPN-(DNA-BD) + SLMAPC-(AD); lane 7, SLMAPC-(DNA-BD) + SLMAPN-(AD); lane 8, SLMAPC-(DNA-BD) + SLMAPC-(AD); lane 9, SLMAPCΔLZ-(DNA-BD) + SLMAPCΔLZ-(AD); lane 10, SLMAPCΔLZ-(DNA-BD) + SLMAPC-(AD); lane 11, SLMAPC-(DNA-BD) + SLMAPCΔLZ (AD); lane 12, ninein-LZ-(DNA-BD) + SLMAPC-(AD); lane 13, ninein-LZ-(AD) + SLMAPC-(DNA-BO) and lane 14, positive control. The level of CAT activity measured for each sample was normalized based on transfection efficiency as described in the Experimental section. SLMAP homodimer formation was mediated by C-terminal sequences (lane 8) encompassing the LZ motifs. Deletion of the LZs (lanes 9–11) failed to activate CAT reporter expression above basal levels. Error bars represent S.D. (**C**) Cells stably expressing either 6Myc-SLMAP1-ΔLZ or the control vector (6Myc-pcDNA3) were cultured in differentiation medium for 6 days, fixed with 4 % PFA and stained with haematoxylin and eosin. Fusion indices were calculated for three independent clones. Error bars represent S.D.

moieties of the T-tubule membrane to organize junctional membrane complexes [44–47]. The ability of SLMAPs to reside in different membrane systems and to homodimerize may allow these molecules to play a role in membrane organization. The structural features of SLMAPs indicate that these molecules belong to a superfamily of tail-anchored membrane proteins and share structural features with syntaxins and synaptobrevins, which function in membrane fusion and excitation–secretion coupling [48–50]. By analogy, our results imply that SLMAPs may regulate myoblast fusion and EC coupling based on their cellular locations and interactions. Topological studies suggest that the SLMAP molecule is cytoplasmically orientated, thus providing the opportunity to assemble with other cytoplasmic, cytoskeletal and membrane components. Protein–protein interactions among membrane and cytoskeletal components represent an important feature of myoblast fusion. For instance, Galliano et al. [51] showed that the interactions between the cytosolic portion of the transmembrane metalloprotease ADAM12 (**A** **D**isintegrin **A**nd **M**etalloproteinase-like 12) and α-actinin are necessary for myoblast fusion. Similarly, the cytoplasmically orientated coiled-coil SLMAP sequences may participate in association with other so far unidentified components of the sarcomeric cytoskeleton or signalling molecules participating in the fusion process. In this regard, our recent results suggest that SLMAP may interact with microtubules and myosin (R. M. Guzzo, unpublished work) and studies are in progress to determine the functional consequences of this interaction in the fusion of myoblasts and in the membrane biology of EC coupling.

B. S. T. was supported by grant #T4619 from the Heart and Stroke Foundation of Ontario and R. M. G. by a Canadian Institutes of Health Research Studentship. We thank Dr Andrew Ridsdale of the Loeb Research Institute (Ottawa, ON, Canada) for his expert technical assistance in confocal microscopy. We also thank Carl MacIntosh and Dr Jackie Vanderluit (University of Ottawa) for their guidance in isolating mouse embryos and Kim Wong (University of Ottawa) for technical assistance with cryostat sectioning.

REFERENCES

1 Bailey, P., Holowacz, T. and Lassar, A. B. (2001) The origin of skeletal muscle stem cells in the embryo and the adult. Curr. Opin. Cell Biol. **13**, 679–689
2 Buckingham, M. (2001) Skeletal muscle formation in vertebrates. Curr. Opin. Genet. Dev. **11**, 440–448
3 Lassar, A. B., Skapek, S. X. and Novitch, A. F. (1994) Regulatory mechanisms that coordinate skeletal muscle differentiation and cell cycle withdrawal. Curr. Opin. Cell Biol. **6**, 788–794
4 Sabourin, L. A. and Rudnicki, M. A. (2000) The molecular regulation of myogenesis. Clin. Genet. **57**, 16–25
5 Pownall, M. E., Gustafsson, M. K. and Emerson, C. P. (2002) Myogenic regulatory factors and the specification of muscle progenitors in vertebrate embryos. Annu. Rev. Cell Dev. Biol. **18**, 747–783
6 Wakelam, M. J. (1985) The fusion of myoblasts. Biochem. J. **228**, 1–12
7 Andres, V. and Walsh, K. (1996) Myogenin expression, cell cycle withdrawal, and phenotypic differentiation are temporally separable events that precede cell fusion upon myogenesis. J. Cell Biol. **132**, 657–666
8 Walsh, K. and Perlman, H. (1997) Cell cycle exit upon myogenic differentiation. Curr. Opin. Genet. Dev. **7**, 597–602
9 Bate, M. (1990) The embryonic development of larval muscles in *Drosophila*. Development **110**, 791–804
10 Paululat, A., Holz, A. and Renkawitz-Pohl, R. (1999) Essential genes for myoblast fusion in *Drosophila* embryogenesis. Mech. Dev. **83**, 17–26
11 Taylor, M. V. (2000) Muscle development: molecules of myoblast fusion. Curr. Biol. **10**, R646–R648
12 Taylor, M. V. (2002) Muscle differentiation: how two cells become one. Curr. Biol. **12**, R224–R228
13 Dworak, H. A. and Sink, H. (2002) Myoblast fusion in *Drosophila*. Bioessays **24**, 591–601
14 Doberstein, S. K., Fetter, R. D., Mehta, A. Y. and Goodman, C. S. (1997) Genetic analysis of myoblast fusion: *blown fuse* is required for progression beyond the prefusion complex. J. Cell Biol. **136**, 1249–1261
15 McDonald, K. A., Lakonishok, M. and Horwitz, A. F. (1995) αv and α3 integrin subunits are associated with myofibrils during myofibrillogenesis. J. Cell Sci. **108**, 2573–2581
16 Yagami-Hiromasa, T., Sato, T., Kurisaki, T., Kamijo, K., Nabeshima, Y. and Fujisawa-Sehara, A. (1995) A metalloprotease-disintegrin participating in myoblast fusion. Nature (London) **377**, 625–656
17 Knudsen, K. A., Myers, L. and McElwee, S. A. (1990) A role for the Ca^{2+}-dependent adhesion molecule, N-cadherin, in myoblast interaction during myogenesis. Exp. Cell Res. **188**, 175–184
18 Knudsen, K. A. (1990) Cell adhesion molecules in myogenesis. Curr. Opin. Cell Biol. **2**, 902–906

19 Zeschnigk, M., Kozian, D., Kuch, C., Schmoll, M. and Starzinski-Powitz, A. (1995) Involvement of M-cadherin in fusion and terminal differentiation of myogenic cells. J. Cell Sci. **108**, 2973–2981
20 Mege, R. M., Goudou, D., Diaz, C., Nicolet, M., Garcia, L., Geraud, G. and Rieger, F. (1992) N-cadherin and N-CAM in myoblast fusion: compared localisation and effect of blockade by peptides and antibodies. J. Cell Sci. **103**, 897–906
21 Franzini-Armstrong, C. (1991) Simultaneous maturation of transverse tubules and sarcoplasmic reticulum during muscle differentiation in the mouse. Dev. Biol. **146**, 353–363
22 Flucher, B. E., Phillips, J. L., Powell, J. A., Andrews, S. B. and Daniels, M. P. (1992) Coordinated development of myofibrils, sarcoplasmic reticulum and transverse tubules in normal and dysgenic mouse skeletal muscle, *in vivo* and *in vitro*. Dev. Biol. **150**, 266–280
23 Flucher, B. E., Takekura, H. and Franzini-Armstrong, C. (1993) Development of the excitation–contraction coupling apparatus in skeletal muscle: association of sarcoplasmic reticulum and transverse tubules with myofibrils. Dev. Biol. **160**, 135–147
24 Takekura, H., Flucher, B. E. and Franzini-Armstrong, C. (2001) Sequential docking, molecular differentiation and positioning of T-tubule–SR junctions in developing mouse skeletal muscle. Dev. Biol. **239**, 204–214
25 Seigneurin-Venin, S., Parrish, E., Marty, I., Rieger, F., Romey, G., Villaz, M. and Garcia, L. (1996) Involvement of the dihydropyridine receptor and internal Ca^{2+} stores in myoblast fusion. Exp. Cell Res. **223**, 301–307
26 Franzini-Armstrong, C. and Jorgensen, A. O. (1994) Structure and development of EC coupling units in skeletal muscle. Annu. Rev. Physiol. **56**, 509–534
27 Flucher, B. E. and Franzini-Armstrong, C. (1996) Formation of junctions involved in excitation–contraction coupling in skeletal and cardiac muscle. Proc. Natl. Acad. Sci. U.S.A. **95**, 8101–8106
28 Wigle, J. T., Demchyshyn, L., Pratt, M. A., Staines, W. A., Salih, M. and Tuana, B. S. (1997) Molecular cloning, expression, and chromosomal assignment of sarcolemmal-associated proteins. A family of acidic amphipathic α-helical proteins associated with the membrane. J. Biol. Chem. **272**, 32384–32394
29 Wielowieyski, P. A., Sevinc, S., Guzzo, R., Salih, M., Wigle, J. T. and Tuana, B. S. (2000) Alternative splicing, expression, and genomic structure of the 3′ region of the gene encoding the sarcolemmal-associated proteins (SLAPs) defines a novel class of coiled-coil tail-anchored membrane proteins. J. Biol. Chem. **275**, 38474–38481
30 Martin, B., Schneider, R., Janetzky, S., Waibler, Z., Pandur, P., Kuhl, M., Behrens, J., von der Mark, K., Starzinski-Powitz, A. and Wixler, V. (2002) The LIM-only protein FHL2 interacts with b-catenin and promotes differentiation of mouse myoblasts. J. Cell Biol. **159**, 113–122
31 Dan, P., Cheung, J. C. Y., Scriven, D. R. L. and Moore, E. D. W. (2003) Epitope-dependent localization of estrogen receptor-a, but not -b, in *en face* arterial endothelium. Am. J. Physiol. Heart Circ. Physiol. **284**, H1295–H1306
32 Yaffe, D. and Saxel, O. (1977) Serial passaging and differentiation of myogenic cells isolated from dystrophic mouse muscle. Nature (London) **270**, 725–727
33 Blau, H. M., Chin, C.-P. and Webster, C. (1983) Cytoplasmic activation of human nuclear genes in stable heterocaryons. Cell (Cambridge, Mass.) **32**, 1171–1180
34 Edmondson, D. G. and Olson, E. N. (1989) A gene with homology to the myc similarity region of MyoD1 is expressed during myogenesis and is sufficient to activate the muscle differentiation program. Genes Dev. **3**, 628–640
35 Wright, W. E., Sassoon, D. A. and Lin, V. K. (1989) Myogenin, a factor regulating myogenesis has a domain homologous to MyoD. Cell (Cambridge, Mass.) **56**, 607–617
36 Hasty, P., Bradley, A., Morris, J. H., Edmondson, D. G., Venuti, J. M., Olson, E. N. and Klein, W. H. (1993) Muscle deficiency and neonatal death in mice with a targeted mutation in the myogenin gene. Nature (London) **364**, 501–506
37 Nabeshima, Y., Hanaoka, K., Hayasaka, M., Esumi, E., Li, S., Nonaka, I. and Nabeshima, Y. (1993) Myogenin gene disruption results in perinatal lethality because of severe muscle defect. Nature (London) **364**, 532–535
38 Landshultz, W. H., Johnson, P. F. and McKnight, S. L. (1988) The leucine zipper: a hypothetical structure common to new class of DNA binding proteins. Science **240**, 1759–1764
39 Adamson, J. G., Zhou, N. E. and Hodges, R. S. (1993) Structure, function and application of the coiled-coil protein folding motif. Curr. Opin. Biotechnol. **4**, 428–437
40 Marx, S. O., Reiken, S., Hisamatsu, Y., Gaburjakova, M., Gaburjakova, J., Yang, Y. M., Rosemblit, N. and Marks, A. R. (2001) Phosphorylation-dependent regulation of ryanodine receptors: a novel role for leucine/isoleucine zippers. J. Cell Biol. **153**, 699–708
41 Hulme, J. T., Ahn, M., Hauschka, S. D., Scheuer, T. and Catterall, W. A. (2002) A novel leucine zipper targets AKAP15 and cyclic AMP-dependent protein kinase to the C-terminus of the skeletal muscle Ca^{++} channel and modulates its function. J. Biol. Chem. **277**, 4079–4087
42 Furst, D. O., Osborn, M. and Weber, K. (1989) Myogenesis in the mouse embryo: differential onset of expression of myogenic proteins and the involvement of titin in myofibril assembly. J. Cell Biol. **109**, 517–527
43 Franzini-Armstrong, C. (1994) The sarcoplasmic reticulum and the transverse tubules. In Myology (Engel, A. E. and Franzini-Armstrong, C., eds.), pp. 176–199, McGraw-Hill, New York
44 Takeshima, H., Komazaki, S., Nishi, M., Iino, M. and Kangawa, K. (2000) Junctophilins: a novel family of junctional membrane complex proteins. Mol. Cell **6**, 11–22
45 Ito, K., Komazaki, S., Sasamoto, K., Yoshida, M., Nishi, M. and Kitamura, K. (2001) Deficiency of triad junction and contraction in mutant skeletal muscle lacking junctophilin type I. J. Cell Biol. **154**, 1059–1067
46 Komazaki, S., Ito, K., Takeshima, H. and Nakamura, H. (2002) Deficiency of triad formation in developing skeletal muscle cells lacking junctophilin type 1. FEBS Lett. **524**, 225–229
47 Komazaki, S., Nishi, M. and Takeshima, H. (2003) Abnormal junctional membrane structures in cardiac myocytes expressing ectopic junctophilin type 1. FEBS Lett. **542**, 69–73
48 Hay, J. C. and Scheller, R. H. (1997) SNAREs and NSF in targeted membrane fusion. Curr. Opin. Cell Biol. **9**, 505–512
49 Jahn, R. and Sudhof, T. C. (1999) Membrane fusion and exocytosis. Annu. Rev. Biochem. **68**, 863–911
50 Jahn, R., Lang, T. and Sudhof, T. C. (2003) Membrane fusion. Cell (Cambridge, Mass.) **112**, 519–533
51 Galliano, M. F., Huet, C., Frygelius, J., Polgren, A., Wewer, U. M. and Engvall, E. (2000) Binding of ADAM12, a marker of skeletal muscle regeneration, to the muscle-specific actin binding protein, α-actinin is required for myoblast fusion. J. Biol. Chem. **275**, 13933–13939
52 Song, K. S., Scherer, P. E., Tang, Z. L., Okamoto, T., Li, S., Chafel, M., Chu, C., Kohtz, D. S. and Lisanti, M. P. (1996) Expression of caveolin-3 in skeletal, cardiac, and smooth muscle cells. Caveolin-3 is a component of the sarcolemma and co-fractionates with dystrophin and dystrophin-associated glycoproteins. J. Biol. Chem. **271**, 15160–15165

Received 12 November 2003/15 March 2004; accepted 15 April 2004
Published as BJ Immediate Publication 15 April 2004, DOI 10.1042/BJ20031723